

Functional Data Analysis with Causation in Observational Studies: Covariate Balancing Functional Propensity Score for Functional Treatments

Xiaoke Zhang¹, Wu Xue¹, and Qiyue Wang²

¹Department of Statistics, George Washington University

²Department of Computer Science, George Washington University

August 21, 2020

Abstract

Functional data analysis, which handles data arising from curves, surfaces, volumes, manifolds and beyond in a variety of scientific fields, is a rapidly developing area in modern statistics and data science in the recent decades. The effect of a functional variable on an outcome is an essential theme in functional data analysis, but a majority of related studies are restricted to correlational effects rather than causal effects. This paper makes the first attempt to study the causal effect of a functional variable as a treatment in observational studies. Despite the lack of a probability density function for the functional treatment, the propensity score is properly defined in terms of a multivariate substitute. Two covariate balancing methods are proposed to estimate the propensity score, which minimize the correlation between the treatment and covariates. The appealing performance of the proposed method in both covariate balance and causal effect estimation is demonstrated by a simulation study. The proposed method is applied to study the causal effect of body shape on human visceral adipose tissue.

Key Words: Functional principal component analysis; Empirical likelihood; Method of moments; Inverse probability weighting.

1 Introduction

Functional data, which arise from curves, surfaces, volumes, manifolds and beyond, are increasingly common in a variety of fields due to recent technological innovations in data collection, data storage and scientific computing. The broad availability of functional datasets and immediate analytic demand have stimulated the rapid development of functional data analysis (FDA) in the past few decades and enhanced its importance in modern statistics and data science. For systematic introductions to FDA and select topics, readers may refer to representative monographs (e.g., [Bosq, 2000](#); [Ferraty and Vieu, 2006](#); [Horváth and Kokoszka, 2012](#); [Hsing and Eubank, 2015](#); [Kokoszka and Reimherr, 2017](#); [Ramsay and Silverman, 2005](#); [Zhang, 2013](#)).

To study the association between a functional predictor and a scalar response, which is a classic topic in FDA, functional regression is the most popular class of approaches (see survey papers, e.g., by [Morris, 2015](#); [Reiss et al., 2017](#)). However, functional regression can only reveal the correlation

between the response and functional predictor, although the causal relationship between those is of primary interest in certain scientific studies. Despite its intellectual merit and practical impact, the research on causal inference in FDA has been inadequate. Among very few existing works, almost all of them focus on either clinical trials or functional variables as covariates (e.g., [Ciarleglio et al., 2015, 2018](#); [Lindquist, 2012](#); [McKeague and Qian, 2014](#); [Miao et al., 2020](#); [Zhao and Luo, 2019](#)). In contrast, we consider a functional variable as a treatment in observational studies.

In the literature on causal inference for observational studies, the causal effect estimation of a binary treatment is a classic topic and has been intensively studied (see reviews, e.g., by [Ding and Li, 2018](#); [Imbens, 2004](#); [Stuart, 2010](#); [Yao et al., 2020](#)). In the past few decades, an increasing number of papers have appeared on multi-level categorical treatments or continuous treatments (e.g., [Fong et al., 2018](#); [Hirano and Imbens, 2004](#); [Imai and Van Dyk, 2004](#); [Imbens, 2000](#); [Kennedy et al., 2017](#); [Li and Li, 2019](#); [Lopez and Gutman, 2017](#); [Robins et al., 2000](#); [Yang et al., 2016](#); [Zhu et al., 2015](#)). Recently, treatments of more complex forms have gradually received more attentions, such as multidimensional categorical treatments (e.g., [D’Amour, 2019](#); [Wang and Blei, 2019](#)) and matrix treatments (e.g., [Yu et al., 2020](#)) among others. To the best of our knowledge, this paper is the first to handle functional treatments in observational data.

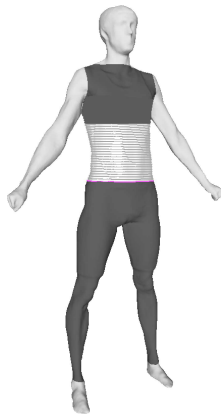


Figure 1: Body circumference over the trunk and two legs of a person sampled at 128 equidistant levels from neck to ankle. The shadeless portion represents the adnominal region.

The practical motivation of this paper is the assessment of human visceral adipose tissue (VAT) using body shape descriptors (e.g., [Samouda et al., 2013](#); [Sun et al., 2017](#); [Wang et al., 2019](#)). VAT is a type of body fat that is stored within the abdominal cavity and located near several vital organs such as liver, stomach, and intestines. Accurate quantitative assessment of VAT is clinically essential since it is known to be associated with the risk for several medial problems, including heart disease, Alzheimer’s disease, type 2 diabetes, stroke, insulin resistance and high cholesterol among others (e.g., [Després, 2007](#); [Jung et al., 2016](#)). Commonly used medical equipments which can provide accurate VAT measurements include dualenergy X-ray absorptiometry (DXA), computed tomography (CT) and magnetic resonance imaging. However, using them is always expensive and reliant on professional operations, and some equipments, e.g., DXA and CT, may expose patients to ionizing radiation (e.g., [Yeh et al., 2009](#)). Due to the prevalence of commodity optical body scan systems, body shape provides a safe and affordable alternative to assessing VAT volume

(e.g., [Ng et al., 2016](#)). Figure 1 provides an illustration of body circumference from neck and ankle, a body shape descriptor extracted from 3D body geometry captured by a commodity level optical body scanner ([Lu et al., 2019](#); [Wang et al., 2019](#)). Apparently body circumference may be regarded as a functional variable of which input is each level between neck and ankle. Following the framework by [Neyman \(1923\)](#) and [Rubin \(1974\)](#), body shape may be regarded as a treatment since people are able to physically intervene it, or parts of it, e.g., via dietary management and exercise, but researchers have so far only focused on its correlation with VAT rather than their causal relationship. In this paper we will fill this void and apply our proposed method to study the causal effect of body shape on VAT.

The main contribution of this paper is twofold. First, the propensity score for functional treatments is properly defined, termed “functional propensity score”, to balance covariates. When a treatment is binary, multi-level categorical or continuous, the propensity score ([Rosenbaum and Rubin, 1983](#)) or generalized propensity score ([Hirano and Imbens, 2004](#); [Imai and Van Dyk, 2004](#); [Imbens, 2000](#)) has been commonly used to balance covariates, which is defined in terms of the conditional mass/density function of the treatment given covariates. However, this way of defining propensity scores is inapplicable to functional treatments since the density function for a functional variable generally does not exist ([Delaigle and Hall, 2010](#)). To circumvent this problem, we propose to substitute the functional treatment by its top functional principal component (FPC) scores, a multivariate variable, and define the functional propensity score by the conditional density function of the FPC scores given covariates. Second, we propose two covariate balancing methods to estimate the functional propensity score. Traditionally the propensity score is estimated by a parametric model together with maximum likelihood, but it is well known that this approach may suffer from model misspecification substantially (e.g., [Kang and Schafer, 2007](#)). To alleviate this drawback, covariate balancing methods with the aim to mimic randomization have been very popular recently (e.g., [Chan et al., 2016](#); [Hainmueller, 2012](#); [Imai and Ratkovic, 2014](#); [Li et al., 2018](#); [Qin and Zhang, 2007](#); [Wong and Chan, 2018](#); [Yiu and Su, 2018](#); [Zhao, 2019](#); [Zubizarreta, 2015](#)). Following the same idea, we seek functional propensity score estimates which can minimize the correlation between the FPC scores and covariates. Our methods generalize the parametric and nonparametric covariate balancing methods by [Fong et al. \(2018\)](#) to estimate the generalized propensity score for continuous treatments, which can improve likelihood-based parametric estimation and avoid parametric misspecification respectively. With a functional propensity score estimate, we fit the outcome model by inverse probability weighting ([Hirano et al., 2003](#); [Robins et al., 2000](#); [Rosenbaum, 1987](#)), which is closely related to the covariate balancing measure.

The rest of the paper proceeds as follows. Section 2 provides the definition of the functional propensity score. In Section 3, two covariate balancing methods are proposed to estimate the functional propensity score, and the causal effect estimation by functional propensity score weighting is also introduced. Section 4 presents a simulation study to evaluate the performances of the two proposed methods with respect to covariate balancing and causal effect estimation accuracy. In Section 5, the proposed methods are applied to study the causal effect of body circumference on VAT. Section 6 concludes the paper.

2 Functional Propensity Score

Let Y be a continuous outcome, the treatment X be a smooth, e.g., twice-differentiable, random function defined on a compact domain \mathcal{T} which is square-integrable, i.e., $E\{\int_{\mathcal{T}} X^2(t) dt\} < \infty$, and

\mathbf{C} be a p -dimensional multivariate covariate with $E(\mathbf{C}^\top \mathbf{C}) < \infty$. Without loss of generality we assume $\mathcal{T} = [0, 1]$, $E\{X(t)\} = 0, t \in [0, 1]$ and $E(\mathbf{C}) = \mathbf{0}$. Suppose that we observe n samples $\{(Y_i, X_i, \mathbf{C}_i) : i = 1, \dots, n\}$ in practice, which are independently and identically distributed (i.i.d.) copies of (Y, X, \mathbf{C}) . For simplicity the trajectories of all $\{X_i : i = 1, \dots, n\}$ are assumed fully observable and uncontaminated by noise. We aim to estimate $E\{Y(x)\}$ in terms of $\{(Y_i, X_i, \mathbf{C}_i) : i = 1, \dots, n\}$, where $x \in L^2 = \{f : \int_0^1 f^2(t) dt < \infty\}$ is any functional value the treatment X can take.

Following the classical causal inference literature, we assume strong ignorability.

Assumption 1 (Strong Ignorability). *Let $Y(x)$ be the potential outcome given the treatment value $X = x$. Assume $X \perp Y(x) \mid \mathbf{C}$ for all $x \in L^2$, where “ \perp ” represents independence.*

The propensity score or generalized propensity score for a categorical or continuous treatment is defined in terms of the conditional probability mass/density function of the treatment given covariates. However, this way of defining the propensity score is inapplicable for functional treatments since the probability density function for a functional variable generally does not exist (Delaigle and Hall, 2010). Therefore we propose to define the propensity score in terms of functional principal component (FPC) scores of the functional treatment.

Explicitly, the Karhunen-Loève theorem allows for the representation $X(t) = \sum_{k=1}^{\infty} A_k \phi_k(t)$, $t \in [0, 1]$, where $\phi_k, k \geq 1$ are eigenfunctions corresponding to the eigenvalues $\lambda_1 \geq \lambda_2 \geq \dots > 0$ of the covariance function $\text{Cov}\{X(s), X(t)\}$. The FPC scores $A_k = \int_0^1 X(t) \phi_k(t) dt, k \geq 1$ are mutually uncorrelated with zero means and $\text{Var}(A_k) = \lambda_k, k \geq 1$. Typically X can be well approximated by the first L summands, i.e., $X(t) \approx \sum_{k=1}^L A_k \phi_k(t)$, where L is often determined such that the top $A_k, k = 1, \dots, L$ cumulatively account for a large proportion of variation of X , e.g., 95% or 99%. Since the majority of X_i 's information can be captured by $\mathbf{A} = (A_1, \dots, A_L)^\top$, we may use \mathbf{A} , a multivariate substitute for X , to define the propensity score. Apparently if X is of finite rank L , then \mathbf{A} can fully capture the information on X .

We next define the propensity score for functional treatments in terms of \mathbf{A} , an L -dimensional substitute of X .

Definition 1 (Functional Propensity Score). *Let r be the conditional probability density function of \mathbf{A} given \mathbf{C} , i.e., $r(\mathbf{a}, \mathbf{c}) = f_{\mathbf{A}|\mathbf{C}}(\mathbf{a} \mid \mathbf{c})$. The rank- L functional propensity score (FPS) is defined by $e_i = r(\mathbf{A}_i, \mathbf{C}_i)$, $i = 1, \dots, n$. The corresponding rank- L FPS weight is defined by $w_i = f_{\mathbf{A}}(\mathbf{A}_i)/e_i, i = 1, \dots, n$, where $f_{\mathbf{A}}(\cdot)$ is the marginal density of \mathbf{A} .*

In practice, one may standardize data before the analysis. Since A_1, \dots, A_L are mutually uncorrelated with $\text{Var}(A_k) = \lambda_k, k = 1, \dots, L$, the standardized \mathbf{A} is $\mathbf{A}^* = (A_1^*, \dots, A_L^*)^\top$ where $A_k^* = \lambda_k^{-1/2} A_k, k = 1, \dots, L$. Let $\mathbf{C}^* = \mathbf{\Gamma}_{\mathbf{C}}^{-1/2} \mathbf{C}$ be the standardized \mathbf{C} where $\mathbf{\Gamma}_{\mathbf{C}} = E(\mathbf{C}\mathbf{C}^\top)$. Similarly for the i th subject, denote $\mathbf{C}_i^* = \mathbf{\Gamma}_{\mathbf{C}}^{-1/2} \mathbf{C}_i$ and $\mathbf{A}_i^* = (A_{i1}^*, \dots, A_{iL}^*)^\top$ where $A_{ik} = \lambda_k^{-1/2} \int_0^1 X_i(t) \phi_k(t) dt, k = 1, \dots, L$. Then the functional propensity score can be alternatively defined in terms of \mathbf{A}^* and \mathbf{C}^* .

Definition 2 (Standardized Functional Propensity Score). *Let r^* be the conditional probability density function of \mathbf{A}^* given \mathbf{C}^* , i.e., $r^*(\mathbf{a}, \mathbf{c}) = f_{\mathbf{A}^*|\mathbf{C}^*}(\mathbf{a} \mid \mathbf{c})$. The rank- L standardized functional*

propensity score (SFPS) is defined by $e_i^* = r^*(\mathbf{A}_i^*, \mathbf{C}_i^*)$, $i = 1, \dots, n$. The corresponding rank- L SFPS weight is $w_i^* = f_{\mathbf{A}^*}(\mathbf{A}_i^*)/e_i^*$, $i = 1, \dots, n$, where $f_{\mathbf{A}^*}(\cdot)$ is the marginal density of \mathbf{A}^* .

We further assume positivity for both FPS and SFPS.

Assumption 2 (Positivity). For r and r^* in Definitions 1 and 2 respectively, assume that $r(\mathbf{a}, \mathbf{C}_i), r^*(\mathbf{a}, \mathbf{C}_i^*) > 0$ for all $\mathbf{a} \in \mathbb{R}^L$.

For simplicity, hereafter we will only use SFPS to remove or mitigate the imbalance between the functional treatment and covariates.

Remark 1.

1. Note that $\phi_k, \lambda_k, A_{ik}, k \geq 1, i = 1, \dots, n$ and $\Gamma_{\mathbf{C}}$ above are population quantities. In practice we can only obtain their sample counterparts, but for brevity we abuse these notations to denote either the population or sample versions depending on their corresponding contexts.
2. In practice functional data are always discretely measured and may be contaminated by noise. For densely measured functional data, one may pre-smooth each function to accurately recover its trajectory (e.g., [Zhang and Chen, 2007](#)) and the FPC scores accordingly.
3. To achieve a satisfactory balance between the functional treatment and covariates, the rank L of both FPS and SFPS is supposed to be sufficiently large such that a majority of the variation of the functional treatment is represented by its top FPC scores. The most commonly used method for selecting L is via the percentage of variance explained by the top FPC scores, which is typically set as 95% or 99%. Note that the selection of L is constrained by the sample size and number of covariates, which will be addressed in Remark 2.

3 Methodology

In this section we propose two covariate balancing methods to estimate the rank- L FPS weights and the corresponding causal effect estimation by FPS weighting.

3.1 SFPS Estimation

Without loss of generality we focus on \mathbf{A}_i^* and \mathbf{C}_i^* , $i = 1, \dots, n$ after standardization. To balance covariates, we seek weights to minimize the weighted correlation between \mathbf{A}_i^* and \mathbf{C}_i^* . By easy calculations we can obtain

$$E w_i^* \mathbf{A}_i^* (\mathbf{C}_i^*)^\top = \mathbf{0}, \quad i = 1, \dots, n. \quad (1)$$

Thus the rank- L SFPS weight $w_i^* = f_{\mathbf{A}^*}(\mathbf{A}_i^*)/f_{\mathbf{A}^*|\mathbf{C}^*}(\mathbf{A}_i^* | \mathbf{C}_i^*)$, $i = 1, \dots, n$ is a minimizer.

Motivated by [Fong et al. \(2018\)](#) who focused on continuous treatments, we consider a parametric and a nonparametric method to estimate rank- L SFPS weights with the covariate balancing condition (1) taken into account.

Parametric SFPS Estimation. To estimate $w_i^* = f_{\mathbf{A}^*}(\mathbf{A}_i^*)/f_{\mathbf{A}^*|\mathbf{C}^*}(\mathbf{A}_i^* | \mathbf{C}_i^*)$, $i = 1, \dots, n$, we assume parametric structures on $f_{\mathbf{A}^*}$ and $f_{\mathbf{A}^*|\mathbf{C}^*}$ and estimate involved unknown parameters. First we assume that \mathbf{A}^* is jointly normal. Then since the components of \mathbf{A}^* , which are standardized FPC scores, are mutually uncorrelated, $f_{\mathbf{A}^*}$ is known as

$$f_{\mathbf{A}^*}(\mathbf{A}_i^*) = (2\pi)^{-L/2} \exp \left\{ -\frac{1}{2} (\mathbf{A}_i^*)^\top (\mathbf{A}_i^*) \right\}.$$

We further assume that \mathbf{A}^* given \mathbf{C}^* is also jointly normal. Then there exist unknown matrices $\boldsymbol{\beta}$ and $\boldsymbol{\Sigma}$ such that

$$\begin{aligned} f_{\mathbf{A}^*|\mathbf{C}^*}(\mathbf{A}_i^* | \mathbf{C}_i^*) &= (2\pi)^{-L/2} \det(\boldsymbol{\Sigma})^{-1/2} \exp \left\{ -\frac{1}{2} (\mathbf{A}_i^* - \boldsymbol{\beta}^\top \mathbf{C}_i^*)^\top \boldsymbol{\Sigma}^{-1} (\mathbf{A}_i^* - \boldsymbol{\beta}^\top \mathbf{C}_i^*) \right\}, \\ \text{so } w_i^* &= \det(\boldsymbol{\Sigma})^{1/2} \exp \left\{ \frac{1}{2} (\mathbf{A}_i^* - \boldsymbol{\beta}^\top \mathbf{C}_i^*)^\top \boldsymbol{\Sigma}^{-1} (\mathbf{A}_i^* - \boldsymbol{\beta}^\top \mathbf{C}_i^*) - \frac{1}{2} (\mathbf{A}_i^*)^\top (\mathbf{A}_i^*) \right\}. \end{aligned} \quad (2)$$

Based on the fact $E(\mathbf{A}_i^* - \boldsymbol{\beta}^\top \mathbf{C}_i^*)(\mathbf{A}_i^* - \boldsymbol{\beta}^\top \mathbf{C}_i^*)^\top = \boldsymbol{\Sigma}$ together with (1), we solve the following method-of-moments equations to estimate the unknown parameters $\boldsymbol{\beta}$ and $\boldsymbol{\Sigma}$:

$$\begin{cases} n^{-1} \sum_{i=1}^n (\mathbf{A}_i^* - \boldsymbol{\beta}^\top \mathbf{C}_i^*)(\mathbf{A}_i^* - \boldsymbol{\beta}^\top \mathbf{C}_i^*)^\top = \boldsymbol{\Sigma}; \\ n^{-1} \sum_{i=1}^n \det(\boldsymbol{\Sigma})^{1/2} \exp \left\{ \frac{1}{2} (\mathbf{A}_i^* - \boldsymbol{\beta}^\top \mathbf{C}_i^*)^\top \boldsymbol{\Sigma}^{-1} (\mathbf{A}_i^* - \boldsymbol{\beta}^\top \mathbf{C}_i^*) - \frac{1}{2} (\mathbf{A}_i^*)^\top (\mathbf{A}_i^*) \right\} \mathbf{A}_i^*(\mathbf{C}_i^*)^\top = \mathbf{0}. \end{cases}$$

With the estimates of $\boldsymbol{\beta}$ and $\boldsymbol{\Sigma}$, w_i^* , $i = 1, \dots, n$ can be estimated following (2).

Nonparametric SFPS Estimation. To avoid possible parametric misspecification for the SFPS, one may adopt the empirical likelihood method ([Owen, 2001](#)) instead where no parametric assumption is needed. Simple calculations can show that $w_i^* = f_{\mathbf{A}^*}(\mathbf{A}_i^*)/f_{\mathbf{A}^*|\mathbf{C}^*}(\mathbf{A}_i^* | \mathbf{C}_i^*)$, $i = 1, \dots, n$ satisfies the four conditions below including (1):

$$E(w_i^*) = 1, \quad E\left\{w_i^* \mathbf{A}_i^*(\mathbf{C}_i^*)^\top\right\} = \mathbf{0}, \quad E(w_i^* \mathbf{A}_i^*) = \mathbf{0}, \quad \text{and } E(w_i^* \mathbf{C}_i^*) = \mathbf{0}, \quad i = 1, \dots, n. \quad (3)$$

Subject to the empirical counterparts of (3), we aim to maximize $\prod_{i=1}^n f_{(\mathbf{A}^*, \mathbf{C}^*)}(\mathbf{A}_i^*, \mathbf{C}_i^*)$, where $f_{(\mathbf{A}^*, \mathbf{C}^*)}$ is the joint density of \mathbf{A}^* and \mathbf{C}^* . Since $f_{(\mathbf{A}^*, \mathbf{C}^*)}(\mathbf{A}_i^*, \mathbf{C}_i^*) = \{f_{\mathbf{A}^*}(\mathbf{A}_i^*)f_{\mathbf{C}^*}(\mathbf{C}_i^*)\}/w_i^*$, an equivalent optimization is

$$\min_{\mathbf{w}^*} \sum_{i=1}^n \log(w_i^*), \quad \text{s.t. } \sum_{i=1}^n w_i^* = n, \quad \sum_{i=1}^n w_i^* \mathbf{A}_i^*(\mathbf{C}_i^*)^\top = \mathbf{0}, \quad \sum_{i=1}^n w_i^* \mathbf{A}_i^* = \mathbf{0}, \quad \sum_{i=1}^n w_i^* \mathbf{C}_i^* = \mathbf{0}, \quad (4)$$

where $\mathbf{w}^* = (w_1^*, \dots, w_n^*)^\top$. By the method of Lagrangian multipliers, it is easy to show that the constrained optimization (4) is equivalent to the unconstrained optimization

$$\max_{\boldsymbol{\gamma}} \sum_{i=1}^n \log(1 - \boldsymbol{\gamma}^\top \mathbf{g}_i), \quad \text{where } \mathbf{g}_i = ((\mathbf{A}_i^*)^\top, (\mathbf{C}_i^*)^\top, \text{vec}(\mathbf{A}_i^*(\mathbf{C}_i^*)^\top)^\top)^\top,$$

with “vec” referring to the vectorization operation, which is unfortunately non-convex.

To resolve this non-convexity issue, we adopt the regularized approach by [Fong et al. \(2018\)](#) which allows for an imbalance between \mathbf{A}_i^* and \mathbf{C}_i^* but meanwhile penalizes such imbalance in the objective function. Explicitly, we consider an ℓ^2 -regularized optimization

$$\begin{aligned} \min_{\mathbf{w}^*, \mathbf{\Gamma}} & \left[\sum_{i=1}^n \log(w_i^*) + \frac{1}{2\rho} \{\text{vec}(\mathbf{\Gamma})\}^\top \{\text{vec}(\mathbf{\Gamma})\} \right], \\ \text{s.t.} \quad & \sum_{i=1}^n w_i^* = n, \quad \frac{1}{n} \sum_{i=1}^n w_i^* \mathbf{A}_i^* (\mathbf{C}_i^*)^\top = \mathbf{\Gamma}, \quad \sum_{i=1}^n w_i^* \mathbf{A}_i^* = \mathbf{0}, \quad \sum_{i=1}^n w_i^* \mathbf{C}_i^* = \mathbf{0}, \end{aligned} \quad (5)$$

where $\rho > 0$ is a tuning parameter. Obviously the constraint $n^{-1} \sum_{i=1}^n w_i^* \mathbf{A}_i^* (\mathbf{C}_i^*)^\top = \mathbf{\Gamma}$ in (5) relaxes the sample counterpart of (1), which allows for an imperfect balance between \mathbf{A}_i^* and \mathbf{C}_i^* . Meanwhile, such imbalance is regularized via an ℓ^2 -penalty and a smaller tuning parameter ρ tends to shrink $\mathbf{\Gamma}$ towards zero.

Note that $\mathbf{\Gamma}$ is a $L \times p$ matrix and the optimization (5) is difficult due to its high dimensionality. To reduce its dimensionality, instead of searching all possible values of $\mathbf{\Gamma}$, we let $\mathbf{\Gamma} = \theta \mathbf{\Gamma}_0$ where $\theta \in [-1, 1]$ is a scalar to be optimized and $\mathbf{\Gamma}_0 = n^{-1} \sum_{i=1}^n \mathbf{A}_i^* (\mathbf{C}_i^*)^\top$ is the unweighted covariance matrix between \mathbf{A}_i^* and \mathbf{C}_i^* . In other words we only consider those weights which can uniformly reduce the entrywise imbalance between \mathbf{A}_i^* and \mathbf{C}_i^* to a certain degree. Accordingly the optimization (5) becomes

$$\begin{aligned} \min_{\mathbf{w}^*, -1 \leq \theta \leq 1} & \left[\sum_{i=1}^n \log(w_i^*) + \frac{\theta^2}{2\rho} \{\text{vec}(\mathbf{\Gamma}_0)\}^\top \{\text{vec}(\mathbf{\Gamma}_0)\} \right], \\ \text{s.t.} \quad & \sum_{i=1}^n w_i^* = n, \quad \frac{1}{n} \sum_{i=1}^n w_i^* \mathbf{A}_i^* (\mathbf{C}_i^*)^\top = \theta \mathbf{\Gamma}_0, \quad \sum_{i=1}^n w_i^* \mathbf{A}_i^* = \mathbf{0}, \quad \sum_{i=1}^n w_i^* \mathbf{C}_i^* = \mathbf{0}, \end{aligned} \quad (6)$$

By the Lagrangian multiplier and profile method, the optimization (6) can be solved by a double-loop routine:

$$\begin{aligned} \text{Inner Loop} & : \quad \hat{\gamma}(\theta) = \arg \max_{\gamma} \sum_{i=1}^n \log \left\{ 1 - \gamma^\top \mathbf{h}_i(\theta) \right\}, \quad \text{for any fixed } \theta \in [-1, 1]; \\ \text{Outer Loop} & : \quad \hat{\theta} = \arg \max_{-1 \leq \theta \leq 1} \left[\sum_{i=1}^n \log \left\{ 1 - \hat{\gamma}(\theta)^\top \mathbf{h}_i(\theta) \right\} - \frac{\theta^2}{2\rho} \{\text{vec}(\mathbf{\Gamma}_0)\}^\top \{\text{vec}(\mathbf{\Gamma}_0)\} \right], \\ & \quad \text{and} \quad \hat{w}_i^* = \frac{1}{1 - \hat{\gamma}(\hat{\theta})^\top \mathbf{h}_i(\hat{\theta})}, \quad i = 1, \dots, n, \end{aligned}$$

where $\mathbf{h}_i(\theta) = ((\mathbf{A}_i^*)^\top, (\mathbf{C}_i^*)^\top, \text{vec}(\mathbf{A}_i^* (\mathbf{C}_i^*)^\top - n\theta \mathbf{\Gamma}_0)^\top)^\top, i = 1, \dots, n$. The inner loop can be solved by the Broyden–Fletcher–Goldfarb–Shanno algorithm while $\hat{\theta}$ in the outer loop can be found by a grid search.

Remark 2.

1. Both parametric and nonparametric SFPS estimation methods above generalize the methods by [Fong et al. \(2018\)](#) for continuous treatments since a functional treatment is degenerated into a continuous treatment if \mathbf{A}^* is one-dimensional, i.e., $L = 1$.

2. As in Remark 1, a large L is preferred to achieve a satisfactory covariate balance, but its practical selection is constrained by the sample size n and the number of covariates p . The parametric method involves estimating β and Σ , of which dimensions are $p \times L$ and $L \times L$ respectively. The nonparametric method involves balancing the covariance matrix between \mathbf{A}^* and \mathbf{C}^* , of which dimension is $L \times p$. Therefore both estimations will be computationally difficult if a too large L is selected.

3. In the nonparametric SFPS estimation, solving (6) involves tuning ρ properly. Generally a suitable ρ should be small since otherwise a large $\hat{\theta}$ is typically obtained, which leads to a liberal imbalance. However, if ρ is extremely small to indicate a very low tolerance of imbalance between \mathbf{A}^* and \mathbf{C}^* , algorithmic convergence is likely to fail, which also leads to a poor covariate balance. Following Fong et al. (2018), we set a default value $\rho = 0.1/n$, but a practitioner may need to explore multiple values to achieve a satisfactory balance.

3.2 Causal Effect Estimation

To estimate the causal effect of the functional treatment on the scalar outcome, one may fit a scalar-on-function outcome model via propensity score weighting. The SFPS weight estimates obtained by either the parametric or nonparametric method in Section 3.1 are used as weights in the involved objective function such that the bias due to the imbalance between the functional treatment and covariates can be substantially reduced.

For example, if the outcome model is assumed a functional linear model

$$E(Y | X) = \mu_0 + \int_0^1 \mu(t)X(t) dt, \quad (7)$$

with the smooth causal effect $\{\mu(t) : t \in [0, 1]\}$ and $\mu_0 = E(Y)$ since $E\{X(t)\} = 0$ for all $t \in [0, 1]$, one may estimate μ is via the following truncation method. Let $\{\psi_k(t) : t \in [0, 1]; k = 1, \dots, L^*\}$ be a set of smooth and orthonormal L^2 basis functions such that $\mu(t) \approx \sum_{k=1}^{L^*} \mu_k \psi_k(t), t \in [0, 1]$ where $\mu_k = \int_0^1 \mu(t) \psi_k(t) dt, k = 1, \dots, L^*$. Then $E(Y | X) \approx \mu_0 + \sum_{k=1}^{L^*} \mu_k \{\int_0^1 X(t) \psi_k(t) dt\}$ and the causal effect can be estimated by $\hat{\mu}(t) = \sum_{k=1}^{L^*} \hat{\mu}_k \psi_k(t), t \in [0, 1]$, where

$$(\hat{\mu}_1, \dots, \hat{\mu}_{L^*}) = \arg \min_{\mu_1, \dots, \mu_{L^*}} \sum_{i=1}^n \hat{w}_i \left(Y_i - \bar{Y} - \sum_{k=1}^{L^*} \mu_k B_{ik} \right)^2, \quad (8)$$

with $\bar{Y} = n^{-1} \sum_{i=1}^n Y_i$, $B_{ik} = \int_0^1 X_i(t) \psi_k(t) dt, k = 1, \dots, L^*, i = 1, \dots, n$, and $\hat{w}_i, i = 1, \dots, n$ being estimated SFPS weights obtained by either the parametric or nonparametric method in Section 3.1.

It is very common that the basis functions $\{\psi_k : k = 1, \dots, L^*\}$ are chosen as the eigenfunctions of X and accordingly $B_{ik}, k = 1, \dots, L^*, i = 1, \dots, n$ are FPC scores. Note that the L^* FPC scores used to fit the outcome model may be chosen independently and differently from those L FPC scores used to define FPS for covariate balancing. Different from L of which selection does not

involve the outcome, the L^* FPC scores used to fit an outcome model may be selected in terms of their predictability of the outcome. We will illustrate this numerically in Section 4 below.

4 Simulation

In this section we present a simulation study to evaluate the numerical performance of the proposed method. We had 200 simulation runs with $n = 200$ independent subjects in each run. The noiseless functional treatment for the i th subject was generated by $X_i(t) = \sum_{k=1}^6 A_{ik}\phi_k(t)$, $t \in [0, 1]$ where the eigenfunctions are $\phi_{2k-1}(t) = \sqrt{2}\sin(2\pi kt)$ and $\phi_{2k}(t) = \sqrt{2}\cos(2\pi kt)$ for $k = 1, 2, 3$, and the FPC scores are $A_{i1} = 4Z_{i1}$, $A_{i2} = 2\sqrt{3}Z_{i2}$, $A_{i3} = 2\sqrt{2}Z_{i3}$, $A_{i4} = 2Z_{i4}$, $A_{i5} = Z_{i5}$, and $A_{i6} = Z_{i6}/\sqrt{2}$, with Z_{i1}, \dots, Z_{i6} independently sampled from the standard normal distribution.

We considered the following four settings to generate the outcome Y_i and a three-dimensional covariate $\mathbf{C}_i = (C_{i1}, C_{i2}, C_{i3})^\top$ depending on whether the FPC scores or outcome are linear in the covariate.

- Setting 1. The covariate was generated by $C_{i1} = Z_{i1} + W_{i1}$, $C_{i2} = 0.2Z_{i2} + W_{i2}$, and $C_{i3} = 0.2Z_{i3} + W_{i3}$ where $W_{i1} \sim N(0, 1)$, $W_{i2} \sim N(0, 0.5)$ and $W_{i3} \sim N(0, 0.5)$ are independent. The outcome was obtained by

$$Y_i = 1 + \int_0^1 \mu(t)X_i(t) dt + 2C_{i1} + e_i,$$

with the true causal effect

$$\mu(t) = 2\sqrt{2}\sin(2\pi t) + \sqrt{2}\cos(2\pi t) + \sqrt{2}\sin(4\pi t)/2 + \sqrt{2}\cos(4\pi t)/2, \quad t \in [0, 1],$$

and the noise $e_i \sim N(0, 25)$. In this setting, both the FPC scores $(A_{i1}, \dots, A_{i6})^\top$ and outcome Y_i are linear in \mathbf{C}_i .

- Setting 2. The covariate was generated by $C_{i1} = (Z_{i1} + 0.5)^2 + W_{i1}$, $C_{i2} = 0.2Z_{i2} + W_{i2}$, and $C_{i3} = 0.2Z_{i3} + W_{i3}$ where $W_{i1} \sim N(0, 1)$, $W_{i2} \sim N(0, 0.5)$ and $W_{i3} \sim N(0, 0.5)$ are independent, so the FPC scores are nonlinear in the covariate. The outcome was generated the same as in Setting 1.
- Setting 3. The covariate was generated in Setting 1. The outcome was obtained by

$$Y_i = 1 + \int_0^1 \mu(t)X_i(t) dt + 2C_{i1} + C_{i2}^2 + e_i,$$

where $e_i \sim N(0, 25)$, so the outcome is nonlinear in the covariate.

- Setting 4. The covariate was generated in Setting 2 while the outcome was generated the same as in Setting 3, so both the FPC scores and outcome are nonlinear in the covariate.

In each setting, the percentage of variance explained (PVE) was set as $\text{PVE}_L = 0.95$ and 0.99 respectively to select L top FPC scores of X to define the rank- L FPS and SFPS. The corresponding SFPS weights were estimated by both the parametric and nonparametric covariate balancing methods in Section 3.1 respectively. The quality of imbalance reduction between the FPC scores and covariate is evaluated by the F-statistic for the linear regression of each selected top FPC score on the covariate, which was fitted by weighted least squares with the estimated SFPS weights obtained by the parametric or nonparametric method. The F-statistic for each linear regression

fitted by ordinary least squares is also given for comparison. The boxplots of these F-statistics are given in Figures 2, 3, 4, and 5.

All four figures demonstrate a substantial and appealing imbalance reduction between the functional treatment and covariate due to either parametric or nonparametric SFPS weighting for both $PVE_L = 0.95$ and 0.99 . The covariate balancing performances of the parametric and nonparametric methods are comparably satisfactory except in a few outlying simulation runs. The parametric method generally outperforms for the top three FPC scores while the nonparametric method is superior for the other FPC scores.

To estimate the causal effect of the functional treatment, the outcome model (7) was fitted by the truncation method in (8) where the weights were the estimated SFPS weights obtained by the parametric or nonparametric method, the basis functions were chosen as the top L^* eigenfunctions for X , and L^* was determined by $PVE_{L^*} = 0.95$ and 0.99 respectively. To assess the accuracy for causal effect estimation, we calculated the integrated squared error (ISE) of each causal effect estimate in each simulation run and further the averaged ISE (AISE) over all simulation runs, together with the median ISE (MISE) due to the presence of outlying estimates. To evaluate the effect of bias removal due to covariate balancing, we computed the integrated squared bias (ISB) using causal effect estimates of all simulation runs. For comparison, all these summary statistics were also provided for causal effect estimates without adjustment between the functional treatment and covariate, each of which was obtained by fitting (8) with all weights being one. These summary statistics for the four simulation settings are given in Tables 1, 2, 3, and 4 respectively.

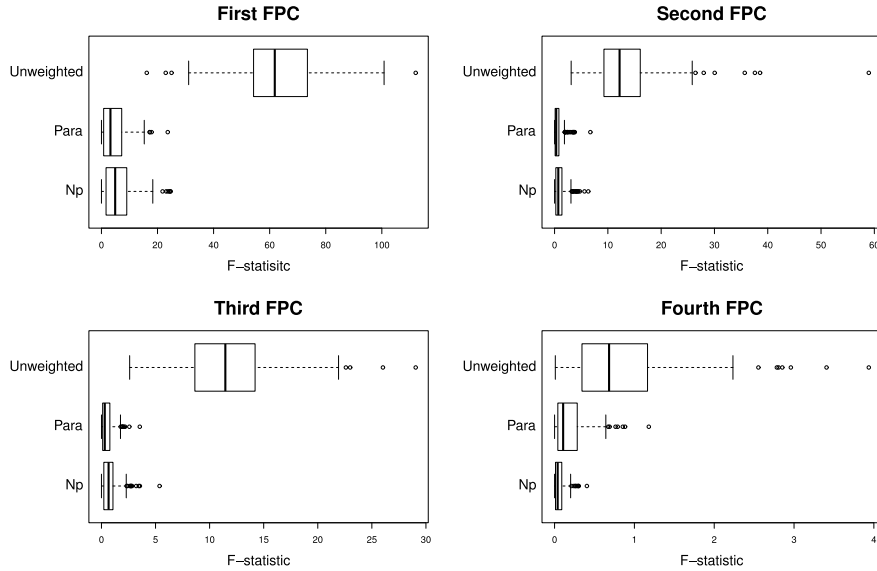


Figure 2: Boxplots of F-statistics for linear regression models of selected top FPC scores on the covariate for Settings 1 and 3. The top FPC scores were selected by $PVE_L = 0.95$. Each linear regression model was fitted by ordinary least squares (Unweighted) or weighted least squares where weights were the estimated SFPS weights obtained by either the parametric (Para) or nonparametric (Np) covariate balancing method.

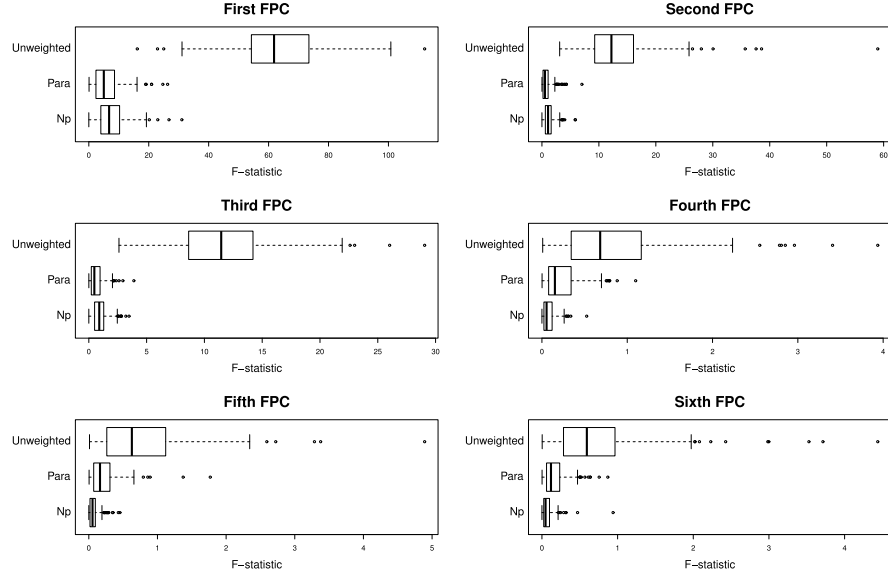


Figure 3: The same as Figure 2 except for $PVE_L = 0.99$. The boxplots for the sixth FPC score were created based on 187 simulation runs while those for the other five FPC scores were based on all 200 simulation runs.

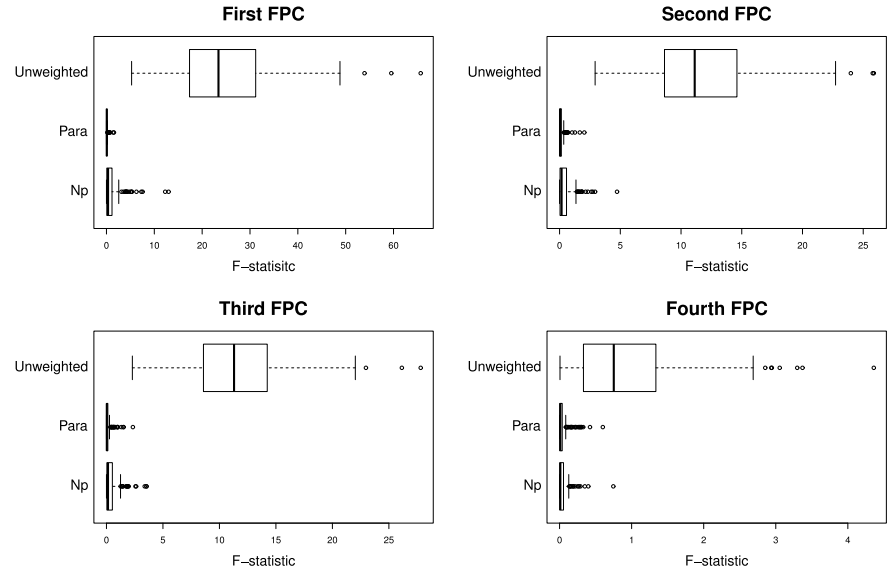


Figure 4: The same as Figure 2 except for Settings 2 and 4.

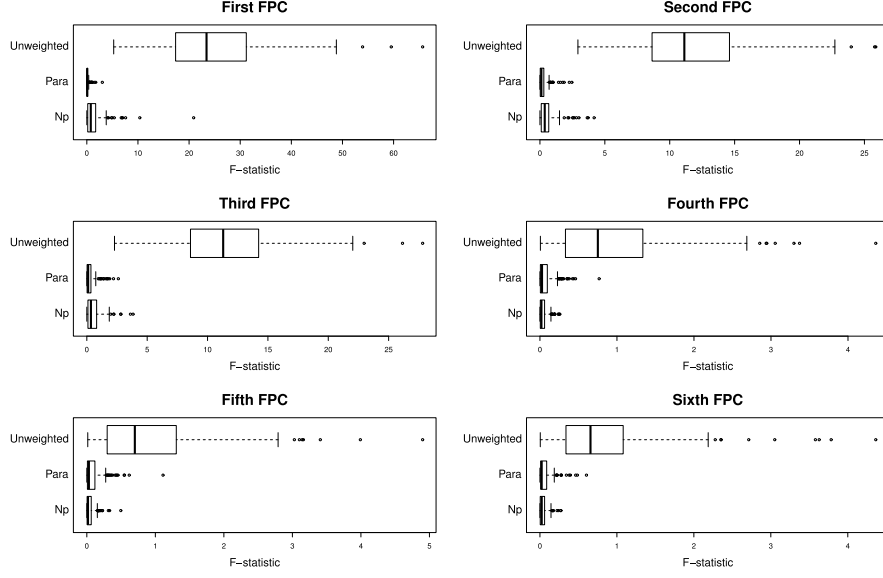


Figure 5: The same as Figure 4 except for $PVE_L = 0.99$. The boxplots for the sixth FPC score were created based on 187 simulation runs while those for the other five FPC scores were based on all 200 simulation runs.

Table 1: Median ISE (MISE), averaged ISE (AISE), and integrated squared bias (ISB) values of causal effect estimates for Setting 1. Each causal effect estimate was obtained by fitting the outcome model (7) using the truncation method in (8) where the weights were all one (Unweighted), the estimated SFPS weights obtained by either the parametric (Para) or nonparametric (Np) covariate balancing method.

		$PVE_{L^*} = 0.95$			$PVE_{L^*} = 0.99$		
		MISE	AISE	ISB	MISE	AISE	ISB
$PVE_L = 0.95$	Unweighted	0.3600	0.3767	0.2968	0.6397	0.7591	0.3042
	Para	0.2263	0.2553	0.0508	1.1476	1.6051	0.0772
	Np	0.1938	0.2262	0.0539	0.8163	1.1478	0.0684
$PVE_L = 0.99$	Para	0.2159	0.2419	0.0631	0.8002	1.1021	0.0987
	Np	0.1943	0.2260	0.0712	0.5937	0.9010	0.0926

As shown in Tables 1, 2, 3, and 4, the ISB values for the causal effect estimators obtained by each covariate balancing method are always much smaller than those for the unadjusted one, which demonstrates the effectiveness of the proposed method to reduce the bias in causal effect estimation.

Table 2: The same as Table 1 except for Setting 2.

		PVE _{L*} = 0.95			PVE _{L*} = 0.99		
		MISE	AISE	ISB	MISE	AISE	ISB
Unweighted		0.3828	0.4143	0.2991	0.7782	0.9333	0.3068
PVE _L = 0.95	Para	0.1421	0.1724	0.0055	1.0200	1.4399	0.0258
	Np	0.1501	0.1885	0.0059	0.9622	1.4393	0.0122
PVE _L = 0.99	Para	0.1252	0.1549	0.0058	0.6571	0.8548	0.0440
	Np	0.1444	0.1688	0.0158	0.5878	0.7998	0.0429

The MISE and AISE values in Tables 1, 2, 3, and 4 show that the causal effect estimation accuracy is influenced by the choices of PVE_L and PVE_{L*}. First, for all three causal effect estimators, using PVE_{L*} = 0.95 to select top L^* FPC scores in the outcome model always leads to a smaller MISE/AISE value and thus a better causal effect estimation than setting PVE_{L*} = 0.99 regardless of the choice of PVE_L. This is somewhat unsurprising since PVE_{L*} = 0.95 selects top $L^* = 4$ FPC scores of X in the outcome model (7), which is correctly specified as implied by the four simulation settings above. In this case, the causal effect estimation accuracies of the two covariate balanced estimators are comparable and substantially better than the unadjusted one. This observation is consistent with the discussion after (8) in Section 3.2 and highlights the importance of outcome model specification.

Table 3: The same as Table 1 except for Setting 3.

		PVE _{L*} = 0.95			PVE _{L*} = 0.99		
		MISE	AISE	ISB	MISE	AISE	ISB
Unweighted		0.3596	0.3788	0.2982	0.6349	0.7617	0.3055
PVE _L = 0.95	Para	0.2269	0.2564	0.0515	1.1306	1.6093	0.0772
	Np	0.1931	0.2281	0.0543	0.8099	1.1474	0.0689
PVE _L = 0.99	Para	0.2182	0.2437	0.0639	0.7905	1.1004	0.0988
	Np	0.2000	0.2277	0.0718	0.5952	0.9004	0.0934

Moreover, for the two adjusted causal effect estimators, selecting top L FPC scores by a larger PVE_L = 0.99 to define SFPS and balance covariates may improve the accuracy for causal effect estimation compared to PVE_L = 0.95. The improvement is substantial if the outcome model is misspecified, i.e., PVE_{L*} = 0.99. When PVE_L = PVE_{L*} = 0.99, in particular, the two adjusted causal effect estimators are more accurate than the unadjusted one in almost all settings. This phenomenon suggests that one use as many FPC scores as possible to define and estimate SFPS weights for the benefit of both reducing imbalance and enhancing causal effect estimation.

Table 4: The same as Table 1 except for Setting 4.

		PVE _{L*} = 0.95			PVE _{L*} = 0.99		
		MISE	AISE	ISB	MISE	AISE	ISB
Unweighted		0.3844	0.4161	0.3005	0.7789	0.9331	0.3081
PVE _L = 0.95	Para	0.1361	0.1754	0.0060	0.9833	1.4363	0.0261
	Np	0.1576	0.1903	0.0061	0.9856	1.4399	0.0127
PVE _L = 0.99	Para	0.1290	0.1572	0.0064	0.6338	0.8561	0.0436
	Np	0.1443	0.1719	0.0161	0.5685	0.8060	0.0437

5 Real Data Application

We applied the proposed parametric and nonparametric covariate balancing methods to the VAT dataset introduced in Section 1 where we aimed to estimate the causal effect of body shape on the VAT-to-weight ratio. The dataset consists of 90 female and 60 male subjects. For each subject, the VAT volume was obtained by a DXA scan and the body circumference sampled at 128 equidistant levels from neck (level 1) to ankle (level 128) was extracted from an optical 3D body scan. See Lu et al. (2019) for more data collection details. Since VAT is stored near organs in the abdominal region, we treated the circumference measured from level 30 (below chest) to level 64 (groin) as the functional treatment X , of which domain incorporates the abdominal region. The multivariate covariate includes ethnicity (white/non-white), the logarithm of height and its square. We centered all variables before the analysis.

Following the suggestion in Section 4 that one use FPC scores as many as possible to define SFPS weights, we selected the top $L = 4$ FPC scores $\mathbf{A} = (A_1, \dots, A_L)^\top$ of the functional treatment by setting $\text{PVE}_L = 0.99$. Their corresponding eigenfunctions are illustrated in Figure 6. Figure 6 shows that the first eigenfunction plays a predominant role in the variation of X with 87.88% explained by the first FPC score, and that along the first eigenfunction, the variation in the upper part of the interested body region is larger than that in the lower part.

To assess the quality of the proposed method in improving covariate balance, we calculated the absolute weighted Pearson correlation between each of the four FPC scores and each covariate where the weight is the estimated SFPS weight obtained by either the parametric (Para) or nonparametric (Np) method. We also computed the unweighted absolute Pearson correlation for comparison. The results are illustrated in Figure 7. As shown in Figure 7, both covariate balancing methods can always reduce the imbalance between the FPC scores and multivariate covariate, and their improvements for the logarithm of height and its square are particularly substantial. The performances of the two methods are comparably satisfactory, although the parametric one is mostly slightly better.

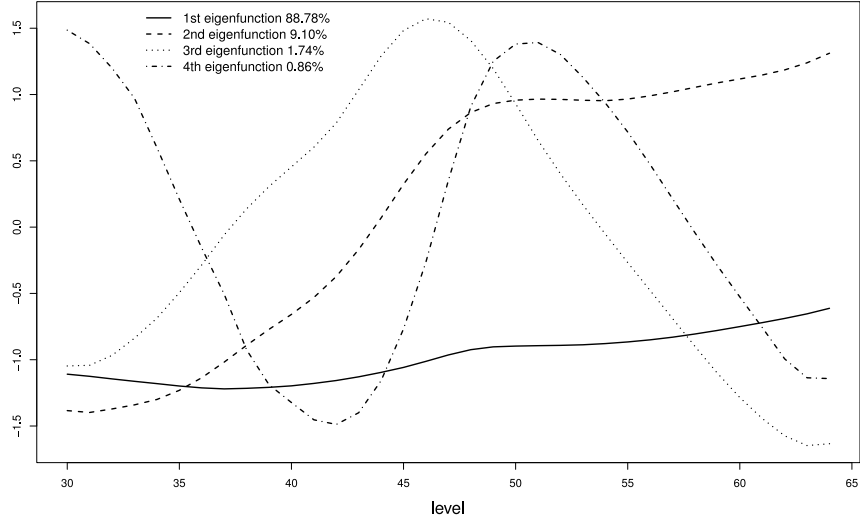


Figure 6: Top four eigenfunctions of the functional treatment and percentages of variation explained by their corresponding FPC scores.

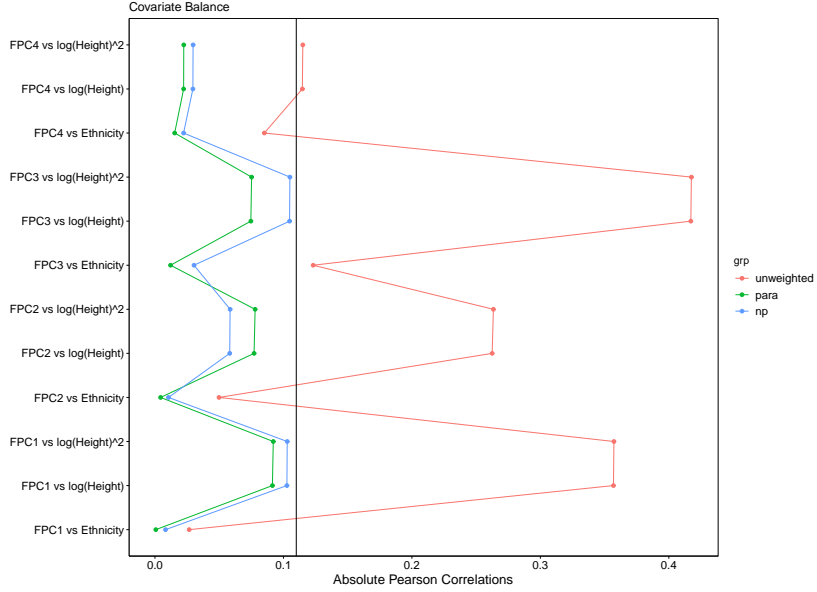


Figure 7: Absolute Pearson correlation between each FPC of the functional treatment and each covariate after weighting by either the parametric (Para) or nonparametric (Np) covariate balancing method. The unweighted absolute Pearson correlation (Unweighted) is also given for comparison.

To estimate the causal effect of body circumference on the VAT-to-weight ratio, we considered a functional linear outcome model which includes X , gender (female= 0/male= 1) and their in-

teraction. To fit the outcome model which involves two unknown coefficient functions for X and interaction term respectively, we followed the same truncation approach in Section 3.2 where both coefficient functions are approximated by a finite number of eigenfunctions of X and the functional linear model is accordingly approximated by a classical linear model on the corresponding FPC scores, gender and their interactions.

Due to the importance of outcome model specification as indicated in Section 4, we adopted the association–variation index (AVI) proposed by Su et al. (2017) to select eigenfunctions/FPC scores of X used in the approximate outcome model. Explicitly the AVI for the k th eigenfunction/FPC score is defined by $V_k = \lambda_k \beta_k^2$, where $\lambda_k = \text{Var}(A_k)$ and $\beta_k = \text{Cov}(A_k, Y)/\text{Var}(A_k)$, $k \geq 1$, which takes into account both the variation of X each FPC score A_k explains and A_k ’s predictability of the outcome Y . For each $k \geq 1$, λ_k may be estimated by the sample variance of $\{A_{ik} : i = 1, \dots, n\}$ and β_k may be estimated by the ordinary least square estimate of the slope when regressing Y on A_k . Following the procedure by Su et al. (2017), we first obtained an initial set of four eigenfunctions/FPC scores by setting PVE = 0.99 together with their estimated AVI values $\hat{V}_k, k = 1, \dots, 4$, and then obtained their sorted AVI values $\hat{V}_{(k)}, k = 1, \dots, 4$ in a decreasing order. Finally we selected the eigenfunction/FPC scores concomitant with the largest three AVI values such that their cumulative percentage of association–variation explained is at least 0.99, that is, $3 = \arg \min_{K \leq 4} \{\sum_{k=1}^K \hat{V}_{(k)} / \sum_{l=1}^4 \hat{V}_{(l)} \geq 0.99\}$. The selected eigenfunctions are the first three in terms of their eigenvalues as illustrated in Figure 6, and their associated FPC scores are used in the approximate outcome model. The results for fitting the approximate outcome model are given in Table 5.

Table 5: Coefficient estimates, standard error (SE) and p-values for fitting the approximate outcome model after weighting by the parametric (Para) and nonparametric (Np) covariate balancing methods respectively. F-statistics for the overall model significance are also given, together with the corresponding p-values based on naïve F-tests which ignore the uncertainty in the process of estimating SFPS weights and selecting FPCs.

	Para			Np		
	Estimate	SE	P-value	Estimate	SE	P-value
Intercept	32.94	2.11	$< 10^{-6}$	32.40	2.23	$< 10^{-6}$
FPC1	-0.22	0.02	$< 10^{-6}$	-0.23	0.02	$< 10^{-6}$
FPC2	-0.36	0.07	1.07×10^{-6}	-0.41	0.07	$< 10^{-6}$
FPC3	0.02	0.14	0.8950	0.10	0.14	0.4550
gender	-17.28	5.99	0.0045	-17.37	5.54	0.0021
FPC1×gender	-0.05	0.04	0.1396	-0.04	0.04	0.2337
FPC2×gender	-0.04	0.15	0.7995	0.01	0.14	0.9712
FPC3×gender	0.04	0.27	0.8748	-0.03	0.24	0.8869
F-statistic=33.38, P-value $< 10^{-6}$			F-statistic=33.62, P-value $< 10^{-6}$			

Table 5 demonstrates an overall significant causal effect of body circumference on VAT-to-weight ratio at the level of significance 0.05 no matter if the covariates are balanced by the parametric or nonparametric method. It also shows that the SFPS weightings by the parametric and nonparametric balancing method lead to almost identical outcome model fitting results.

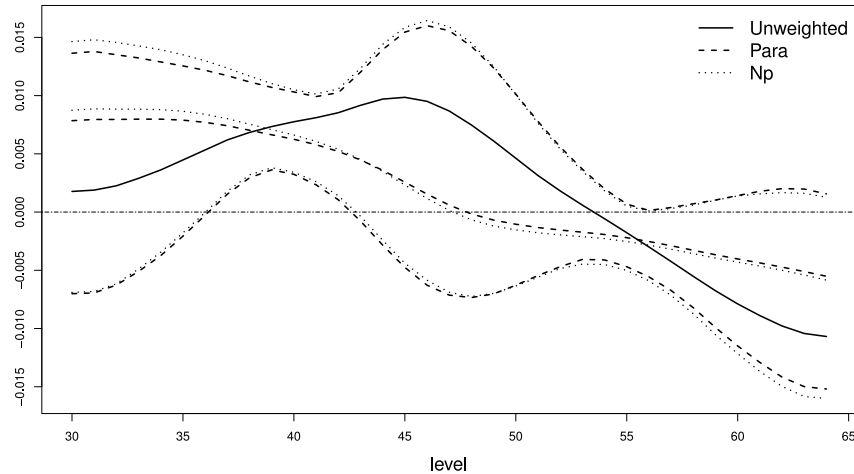


Figure 8: Estimated causal effects of body circumference on VAT-to-weight ratio for female subjects where the multivariate covariate is either unadjusted (Unweighted) or adjusted for by the parametric (Para) or nonparametric (Np) covariate balancing method. The 99% bootstrap pointwise confidence intervals are given for the two covariate balanced casual effect estimates.

The estimated causal effects of body circumference for females, males and their difference are illustrated in Figures 8, 9 and 10 respectively, together with their 99% pointwise confidence intervals based on 10,000 bootstrap samples. Similar to the observation from Table 5, all three figures show that the parametric and nonparametric covariate balancing methods lead to very similar causal effect estimates. They also show that the unadjusted estimates seem to be seriously biased for the causal effect for females (Figure 8) and the causal effect difference between males and females (Figure 10), but not for the causal effect for males (Figure 9).

Figure 8 shows that the causal effect of body circumference on VAT-to-weight ratio is overall significant for females no matter if the covariates are balanced by the parametric or nonparametric method. This can be validated by p -values < 0.0001 based on naïve F-tests which ignore the uncertainty in the process of selecting FPCs and estimating SFPS weights. The domain for the significant causal effect is between levels 36 and 43, which approximately corresponds to the body region below chest to navel, and the causal effect gradually decreases from level 36 to level 43. Figure 9 shows that the causal effect of body circumference for males is also overall significant, with p -values < 0.0001 by naïve F-tests. The significant domain for the causal effect is essentially the same as that for females, but the causal effect tends to slightly increase from level 36 to level 43. Despite the seeming different causal effect patterns between females and males, Figure 10 shows no significant difference in the causal effect of body circumference between the two gender groups,

with p-values 0.5274 (Para) and 0.6538 (Np) respectively by naïve F-tests.

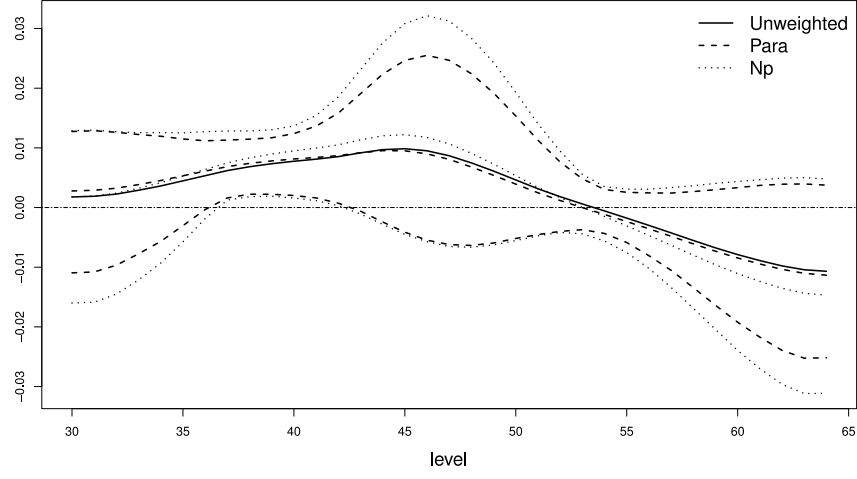


Figure 9: The same as Figure 8 except for the causal effect for males.

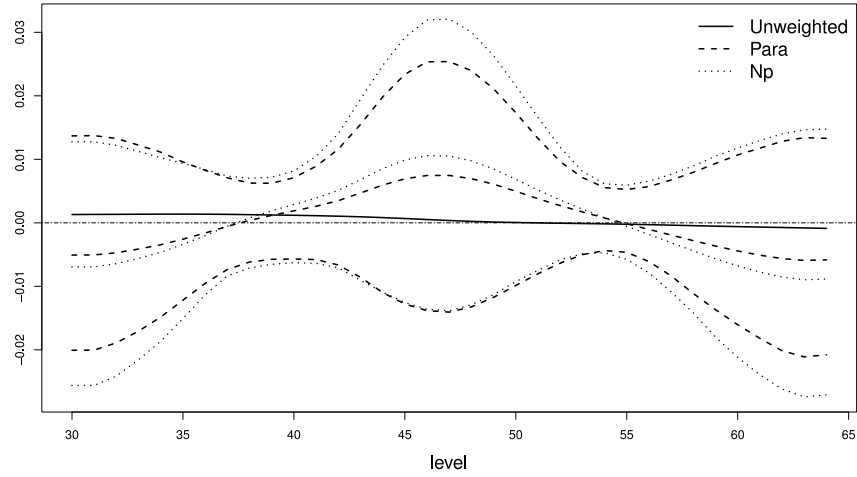


Figure 10: The same as Figure 8 except for the causal effect difference between males and females.

6 Discussion

To the best of our knowledge, this paper is the first to study the causal effect estimation of functional treatments in observational studies. Due to the lack of a probability density function for a functional variable in general, we properly define the FPS in terms of a multivariate substitute for the functional treatment, i.e., its FPC scores. We propose two covariate balancing methods to

estimate the FPS weights, which are used in an outcome model to estimate the causal effect by FPS weighting. The appealing numerical performance of the proposed method in both imbalance reduction and causal effect estimation accuracy is demonstrated by a simulation study. Using the proposed method, the paper has made the first endeavor to study the causal effect of body circumference on VAT among all body-shape-based analyses of VAT.

The proposed method may be straightforwardly generalizable to other scenarios. For example, it is almost directly applicable to handle multidimensional continuous treatments (e.g., Kong et al., 2019) and functional/categorical outcomes. If the covariate set consists of a functional variable, the proposed method is also applicable by including its top FPC scores in \mathbf{C} (e.g., Miao et al., 2020). With slight modifications, the proposed method may be used to study the joint causal effect of multiple functional treatments if the FPS and SFPS are defined in terms of their joint FPC scores obtained by multivariate functional principal component analysis (e.g., Chiou et al., 2014; Happ and Greven, 2018).

This paper has a few limitations which are worthy of future studies. First, the proposed method relies on the FPC scores of the functional treatment. A consistent recovery of them is attainable if the functional treatment is fully observed or densely measured, but not if it is sparsely and irregularly measured (e.g., Yao et al., 2005). A future research topic is to develop causal effect estimation methods for sparsely and irregularly observed functional treatments. Moreover, it is worthwhile to study the numerical improvements on both parametric and nonparametric methods for FPS estimation since they may lead to a poor covariate balance if a large number of FPC scores is selected or the number of covariates is moderate or large. Another interesting research direction is to study non-truncation methods for outcome model fitting, e.g., via roughness regularization.

Acknowledgements

The research of Xiaoke Zhang was partially supported by the USA National Science Foundation under grant DMS-1832046. We are thankful for Dr. James K. Hahn who kindly provides the VAT dataset.

References

- Bosq, D. (2000). *Linear processes in function spaces: theory and applications*, Volume 149. Springer, New York.
- Chan, K. C. G., S. C. P. Yam, and Z. Zhang (2016). Globally efficient non-parametric inference of average treatment effects by empirical balancing calibration weighting. *Journal of the Royal Statistical Society: Series B (Statistical Methodology)* 78(3), 673–700.
- Chiou, J.-M., Y.-T. Chen, and Y.-F. Yang (2014). Multivariate functional principal component analysis: a normalization approach. *Statistica Sinica* 24(4), 1571–1596.
- Ciarleglio, A., E. Petkova, R. T. Ogden, and T. Tarpey (2015). Treatment decisions based on scalar and functional baseline covariates. *Biometrics* 71(4), 884–894.
- Ciarleglio, A., E. Petkova, T. Ogden, and T. Tarpey (2018). Constructing treatment decision rules based on scalar and functional predictors when moderators of treatment effect are unknown. *Journal of the Royal Statistical Society: Series C (Applied Statistics)* 67(5), 1331–1356.

- D’Amour, A. (2019). On multi-cause approaches to causal inference with unobserved confounding: Two cautionary failure cases and a promising alternative. In *The 22nd International Conference on Artificial Intelligence and Statistics*, pp. 3478–3486.
- Delaigle, A. and P. Hall (2010). Defining probability density for a distribution of random functions. *The Annals of Statistics* 38(2), 1171–1193.
- Després, J.-P. (2007). Cardiovascular disease under the influence of excess visceral fat. *Critical Pathways in Cardiology* 6(2), 51–59.
- Ding, P. and F. Li (2018). Causal inference: a missing data perspective. *Statistical Science* 33(2), 214–237.
- Ferraty, F. and P. Vieu (2006). *Nonparametric functional data analysis: theory and practice*. Springer, New York.
- Fong, C., C. Hazlett, and K. Imai (2018). Covariate balancing propensity score for a continuous treatment: Application to the efficacy of political advertisements. *The Annals of Applied Statistics* 12(1), 156–177.
- Hainmueller, J. (2012). Entropy balancing for causal effects: A multivariate reweighting method to produce balanced samples in observational studies. *Political Analysis* 20(1), 25–46.
- Happ, C. and S. Greven (2018). Multivariate functional principal component analysis for data observed on different (dimensional) domains. *Journal of the American Statistical Association* 113(522), 649–659.
- Hirano, K. and G. W. Imbens (2004). The propensity score with continuous treatments. In *Applied Bayesian Modeling and Causal Inference from Incomplete-Data Perspectives: An Essential Journey with Donald Rubin’s Statistical Family*, pp. 73–84. Wiley Online Library.
- Hirano, K., G. W. Imbens, and G. Ridder (2003). Efficient estimation of average treatment effects using the estimated propensity score. *Econometrica* 71(4), 1161–1189.
- Horváth, L. and P. Kokoszka (2012). *Inference for functional data with applications*, Volume 200. Springer, New York.
- Hsing, T. and R. Eubank (2015). *Theoretical foundations of functional data analysis, with an introduction to linear operators*. John Wiley & Sons.
- Imai, K. and M. Ratkovic (2014). Covariate balancing propensity score. *Journal of the Royal Statistical Society: Series B (Statistical Methodology)* 76(1), 243–263.
- Imai, K. and D. A. Van Dyk (2004). Causal inference with general treatment regimes: Generalizing the propensity score. *Journal of the American Statistical Association* 99(467), 854–866.
- Imbens, G. W. (2000). The role of the propensity score in estimating dose-response functions. *Biometrika* 87(3), 706–710.
- Imbens, G. W. (2004). Nonparametric estimation of average treatment effects under exogeneity: A review. *Review of Economics and Statistics* 86(1), 4–29.

- Jung, S. H., K. H. Ha, and D. J. Kim (2016). Visceral fat mass has stronger associations with diabetes and prediabetes than other anthropometric obesity indicators among korean adults. *Yonsei Medical Journal* 57(3), 674–680.
- Kang, J. D. Y. and J. L. Schafer (2007). Demystifying double robustness: A comparison of alternative strategies for estimating a population mean from incomplete data. *Statistical Science* 22(4), 523–539.
- Kennedy, E. H., Z. Ma, M. D. McHugh, and D. S. Small (2017). Nonparametric methods for doubly robust estimation of continuous treatment effects. *Journal of the Royal Statistical Society: Series B (Statistical Methodology)* 79(4), 1229–1245.
- Kokoszka, P. and M. Reimherr (2017). *Introduction to functional data analysis*. CRC Press.
- Kong, D., S. Yang, and L. Wang (2019). Multi-cause causal inference with unmeasured confounding and binary outcome. arXiv preprint arXiv:1907.13323.
- Li, F. and F. Li (2019). Propensity score weighting for causal inference with multiple treatments. *The Annals of Applied Statistics* 13(4), 2389–2415.
- Li, F., K. L. Morgan, and A. M. Zaslavsky (2018). Balancing covariates via propensity score weighting. *Journal of the American Statistical Association* 113(521), 390–400.
- Lindquist, M. A. (2012). Functional causal mediation analysis with an application to brain connectivity. *Journal of the American Statistical Association* 107(500), 1297–1309.
- Lopez, M. J. and R. Gutman (2017). Estimation of causal effects with multiple treatments: a review and new ideas. *Statistical Science* 32(3), 432–454.
- Lu, Y., J. K. Hahn, and X. Zhang (2019). 3d shape-based body composition inference model using a bayesian network. *IEEE Journal of Biomedical and Health Informatics* 24(1), 205–213.
- McKeague, I. W. and M. Qian (2014). Estimation of treatment policies based on functional predictors. *Statistica Sinica* 24(3), 1461–1485.
- Miao, R., W. Xue, and X. Zhang (2020). Average treatment effect estimation in observational studies with functional covariates. arXiv preprint arXiv:2004.06166.
- Morris, J. S. (2015). Functional regression. *Annual Review of Statistics and Its Application* 2(1), 321–359.
- Neyman, J. (1923). Sur les applications de la théorie des probabilités aux expériences agricoles: Essai des principes. *Roczniki Nauk Rolniczych* 10, 1–51.
- Ng, B., B. Hinton, B. Fan, A. Kanaya, and J. Shepherd (2016). Clinical anthropometrics and body composition from 3d whole-body surface scans. *European Journal of Clinical Nutrition* 70(11), 1265–1270.
- Owen, A. B. (2001). *Empirical likelihood*. Chapman and Hall/CRC.

- Qin, J. and B. Zhang (2007). Empirical-likelihood-based inference in missing response problems and its application in observational studies. *Journal of the Royal Statistical Society: Series B (Statistical Methodology)* 69(1), 101–122.
- Ramsay, J. O. and B. W. Silverman (2005). *Functional data analysis* (2nd ed.). New York: Springer.
- Reiss, P. T., J. Goldsmith, H. L. Shang, and R. T. Ogden (2017). Methods for scalar-on-function regression. *International Statistical Review* 85(2), 228–249.
- Robins, J. M., M. Á. Hernán, and B. Brumback (2000). Marginal structural models and causal inference in epidemiology. *Epidemiology* 11(5), 550–560.
- Rosenbaum, P. R. (1987). Model-based direct adjustment. *Journal of the American Statistical Association* 82(398), 387–394.
- Rosenbaum, P. R. and D. B. Rubin (1983). The central role of the propensity score in observational studies for causal effects. *Biometrika* 70(1), 41–55.
- Rubin, D. B. (1974). Estimating causal effects of treatments in randomized and nonrandomized studies. *Journal of Educational Psychology* 66(5), 688–701.
- Samouda, H., A. Dutour, K. Chaumoitre, M. Panuel, O. Dutour, and F. Dadoun (2013). Vat=taat-saat: Innovative anthropometric model to predict visceral adipose tissue without resort to ct-scan or dxa. *Obesity* 21(1), E41–E50.
- Stuart, E. A. (2010). Matching methods for causal inference: a review and a look forward. *Statistical Science* 25(1), 1–21.
- Su, Y.-R., C.-Z. Di, and L. Hsu (2017). Hypothesis testing in functional linear models. *Biometrics* 73(2), 551–561.
- Sun, J., B. Xu, J. Lee, and J. H. Freeland-Graves (2017). Novel body shape descriptors for abdominal adiposity prediction using magnetic resonance images and stereovision body images. *Obesity* 25(10), 1795–1801.
- Wang, Q., Y. Lu, X. Zhang, and J. K. Hahn (2019). A novel hybrid model for visceral adipose tissue prediction using shape descriptors. In *The 41st Annual International Conference of the IEEE Engineering in Medicine and Biology Society (EMBC)*, pp. 1729–1732. IEEE.
- Wang, Y. and D. M. Blei (2019). The blessings of multiple causes. *Journal of the American Statistical Association* 114(528), 1574–1596.
- Wong, R. K. W. and K. C. G. Chan (2018). Kernel-based covariate functional balancing for observational studies. *Biometrika* 105(1), 199–213.
- Yang, S., G. W. Imbens, Z. Cui, D. E. Faries, and Z. Kadziola (2016). Propensity score matching and subclassification in observational studies with multi-level treatments. *Biometrics* 72(4), 1055–1065.
- Yao, F., H.-G. Müller, and J.-L. Wang (2005). Functional data analysis for sparse longitudinal data. *Journal of the American Statistical Association* 100(470), 577–590.

- Yao, L., Z. Chu, S. Li, Y. Li, J. Gao, and A. Zhang (2020). A survey on causal inference. arXiv preprint arXiv:2002.02770.
- Yeh, B. M., J. A. Shepherd, Z. J. Wang, H. Seong Teh, R. P. Hartman, and S. Prevrhal (2009). Dual-energy and low-kvp ct in the abdomen. *American Journal of Roentgenology* 193(1), 47–54.
- Yiu, S. and L. Su (2018). Covariate association eliminating weights: a unified weighting framework for causal effect estimation. *Biometrika* 105(3), 709–722.
- Yu, D., L. Wang, D. Kong, and H. Zhu (2020). Beyond scalar treatment: A causal analysis of hippocampal atrophy on behavioral deficits in alzheimer’s studies. arXiv preprint arXiv:2007.04558.
- Zhang, J.-T. (2013). *Analysis of variance for functional data*. Chapman and Hall/CRC.
- Zhang, J.-T. and J. Chen (2007). Statistical inferences for functional data. *The Annals of Statistics* 35(3), 1052–1079.
- Zhao, Q. (2019). Covariate balancing propensity score by tailored loss functions. *The Annals of Statistics* 47(2), 965–993.
- Zhao, Y. and X. Luo (2019). Granger mediation analysis of multiple time series with an application to functional magnetic resonance imaging. *Biometrics* 75(3), 788–798.
- Zhu, Y., D. L. Coffman, and D. Ghosh (2015). A boosting algorithm for estimating generalized propensity scores with continuous treatments. *Journal of Causal Inference* 3(1), 25–40.
- Zubizarreta, J. R. (2015). Stable weights that balance covariates for estimation with incomplete outcome data. *Journal of the American Statistical Association* 110(511), 910–922.